

# The effect of phosphate coatings on carbon steel protection from corrosion in a chloride-contaminated alkaline solution

**Olga Girčienė\***,

**Rimantas Ramanauskas,**

**Laima Gudavičiūtė,**

**Aldona Martušienė**

*Institute of Chemistry,  
Centre for Physical  
Sciences and Technology,  
Goštauto St. 9,  
LT-01108 Vilnius,  
Lithuania*

The protective abilities of four crystalline Zn (PZn), Zn-Ca (PZnCa), Zn-Ni (PZnNi) and Zn-Ni-Mn (PZnNiMn) phosphate coatings on carbon steel in a chloride-contaminated alkaline solution have been studied. The chemical composition and the morphology of the phosphate coating were evaluated by the X-ray diffraction (XRD) and scanning electron microscopy (SEM) techniques, while the corrosion and porosity parameters of samples were determined by electrochemical measurements. According to XRD analysis data all investigated coatings were composed of three phases: hopeite  $\text{Zn}_3(\text{PO}_4)_2 \cdot 4\text{H}_2\text{O}$ , phosphophyllite  $\text{Zn}_2\text{Fe}(\text{PO}_4)_2 \cdot 4\text{H}_2\text{O}$  and the substrate metal Fe. The results of electrochemical measurements revealed that after immersion into a saturated  $\text{Ca}(\text{OH})_2 + 1 \text{ M NaCl}$  solution for 1 h carbon steel samples covered with the phosphate coatings possessed from four- to seventeen-fold higher  $R_p$  values in comparison to those of bare steel samples. The porosity values obtained by electrochemical impedance spectroscopy (EIS) were in total agreement with the values evaluated by linear polarization measurements. To summarize the results of measurements, the low porosity medium weight PZnNiMn coating on carbon steel demonstrated effective protective properties in the chloride-contaminated alkaline solution.

**Key words:** carbon steel, phosphate coating, porosity, corrosion resistance

## INTRODUCTION

Steel bars embedded in concrete are protected from corrosion by a thin oxide layer formed on their surfaces because of highly alkaline environment of the surrounding concrete ( $\text{pH} \approx 13$ ). However, the breakdown of the passive film and hence the corrosion can be stimulated either due to carbonisation of concrete, which reduces pH of pore water to a non-protective level, or by the presence of significant quantities of chloride ions at reinforcement level in concrete. The most important cause of corrosion initiation in steel bars is the ingress of  $\text{Cl}^-$  ions to the steel surface. Chlorides may depassivate steel, even at high pH [1–4]. A variety of protective methods have

been used to improve the corrosion resistance of reinforcing bars. Application of phosphate coatings could be one of them [5–7].

The phosphating of metals is a traditional surface treatment technique used for various applications in different industrial fields [8–11]. The mechanism of phosphate coatings formation is quite complex, but for all processes based on heavy metal phosphate solutions it depends on the following basic equilibrium [11]:



Phosphating is essentially an electrochemical phenomenon in which dissolution of the metal occurs at the micro-

\* Corresponding author. E-mail: olgag@chi.lt

anode(s) and discharge of hydrogen followed by hydrolysis and precipitation of insoluble phosphates takes place at the micro-cathode(s).

Zn phosphate coatings on Zn consist essentially of  $Zn_3(PO_4)_2 \cdot 4H_2O$  (hopeite). Only in the case of formation of a Zn phosphate coating on Zn the reaction is simple and the composition of the coating is straightforward. With Zn phosphate coating on a steel substrate the situation becomes more complex. The presence of zinc iron phosphate,  $Zn_2Fe(PO_4)_2 \cdot 4H_2O$  (phosphophyllite), in zinc phosphate coatings has been demonstrated by several workers [10, 11]. Under conditions of minimum agitation a high concentration of ferrous ions can accumulate at the metal-solution interface and these are then available for redeposition in the zinc iron phosphate.

The addition of cations, such as Ca, Mn and Ni, to the  $Zn_3(PO_4)_2 \cdot 4H_2O$  is an alternative to improve the resistance of the phosphate coatings in alkaline and acid environments. The extensive reviews on various aspects of phosphate coatings are given in [5, 8–16]. Films from Ca modified Zn phosphate baths contain rhombic crystals of scholzite  $Zn_2Ca(PO_4)_2 \cdot 2H_2O$ , the proportion of the latter being directly related to the Ca content in the solution [11]. The presence of  $Ni^{2+}$  ions in the phosphating bath improves the corrosion resistance at the base of pores [17, 18] and accelerates the surface reactions during phosphating [19]. The increase in phosphate layer mass with increase in Ni concentration was reported in the literature [18]. Mn addition to the bath improves the corrosion resistance and decreases the porosity by formation of a dense and fine microstructure [20, 21].

The literature data show that the alkaline stability of phosphate coatings depends on their chemical composition and their crystal structure [5, 13, 14, 22]. The elements such as Ni and Mn are used to increase the alkaline stability of phosphate layers [13, 14, 21].

The main problem in application of phosphate coatings in aggressive media is the existence of open pores and pinholes [8, 12, 23, 24]. The corrosion resistance of the phosphate coating is related to the size and population density of pores in the film. The pores provide a path for corrosion attack, leading to localise corrosion in an aggressive environment. As the corrosion reactions are initiated at the coating-substrate interface, determination of porosity is important to estimate the overall corrosion resistance of the coated materials [23].

The corrosion of steel in concrete is difficult to investigate, mainly because of experimental problems such as the electrode and cell designs (e. g. position of the reference and counter electrodes), a large potential drop in concrete and its compensation, the development of macro-corrosion cells, etc. An alternative way of tackling the problem is to use

solutions that simulate the chemical environment present in the pores of concrete. Since the pore solutions in cement and concrete are thought to consist mainly of aqueous potassium hydroxide (KOH), sodium hydroxide (NaOH), and calcium hydroxide ( $Ca(OH)_2$ ), it is possible that the studies of electrochemical behaviour of carbon steel in these solutions could be useful as a basis for understanding the electrochemical corrosion behaviour of steel reinforcement in porous concrete structures.

The aim of the present work was to investigate the protective abilities of Zn (PZn), Zn-Ca (PZnCa), Zn-Ni (PZnNi) and Zn-Ni-Mn (PZnNiMn) phosphate coatings on carbon steel in chloride contaminated alkaline solutions.

## EXPERIMENTAL

### Substrate and coatings

Carbon steel samples with an area of 4 cm<sup>2</sup>, the composition of which is listed in Table 1, covered with the phosphate layers were used as the working electrodes. The phosphating processes primarily included pre-cleaning, activation, phosphating and post-rinsing. Four types of phosphating solutions were used for coating formation under the conditions: PZn ( $Zn^{2+} - 0.13$  M,  $PO_4^{3-} - 0.3$  M,  $NO_3^- - 0.18$  M,  $NO_2^- - 0.0025$  M, pH = 2.2–2.5, t = 45–55 °C, 10 min), PZnCa ( $Zn^{2+} - 0.08$  M,  $Ca^{2+} - 0.04$  M,  $PO_4^{3-} - 0.2$  M,  $NO_3^- - 0.16$  M,  $NO_2^- - 0.0025$  M, pH = 2.2–2.5, t = 45–55 °C, 10 min), PZnNi ( $Zn^{2+} - 0.16$  M,  $Ni^{2+} - 0.036$  M,  $PO_4^{3-} - 0.42$  M,  $NO_3^- - 0.28$  M, pH = 2.2–2.5, t = 45–55 °C, 10 min), PZnNiMn ( $Zn^{2+} - 0.04$  M,  $Mn^{2+} - 0.028$  M,  $Ni^{2+} - 0.016$  M,  $PO_4^{3-} - 0.26$  M,  $NO_3^- - 0.1$  M, pH = 3.2–3.6, t = 50–55 °C, 10 min). The phosphated samples were kept for 3 days under ambient conditions prior to the measurements.

### Morphology and composition

The morphology and elemental composition of the phosphate coating were studied by a scanning electron microscope (SEM) EVO 50 EP (Carl Zeiss SMT AG) with an INCA energy disperse X-ray (EDX) spectrometer (Oxford Instruments).

The phases in the phosphate coating were determined by X-ray diffraction (XRD) measurements, which were performed with a diffractometer D8 Advance (Bruker AXS) equipped with a Göbel mirror (primary beam monochromator) for Cu radiation ( $\lambda = 0.154183$  nm). The step-scan mode was used in the  $2\theta$  ranges from  $xx^\circ$  to  $yy^\circ$  with a step-length of  $0.04^\circ$  and a counting time of 5 s per step.

### Electrochemical measurements

The corrosion behaviour of phosphated carbon steel was investigated in an aerated stagnant saturated  $Ca(OH)_2$  solution containing 1 M NaCl. The electrolyte was prepared

Table 1. Chemical composition of the steel (wt. %)

Elements	C	Mn	Si	Cr	Ni	Cu	P	S
Composition	0.21	1.2	0.6	≤0.3	<0.3	<0.3	<0.04	<0.045

from analytical grade chemicals and deionised water. All the experiments were performed at ambient temperature.

The working electrodes were carbon steel samples covered with the phosphate layers (Table 2).

All electrochemical measurements were performed with an Autolab PGSTAT302 potentiostat using a standard three-electrode system with a Pt counter electrode and a saturated Ag/AgCl reference electrode. All potentials are reported versus a saturated Ag/AgCl reference electrode. Before experiments, the open circuit potential ( $E_{\text{corr}}$ ) of electrodes in the solution was monitored for 1 h. The data on  $E_{\text{corr}}$  values were average of five measurements. The corrosion current densities ( $i_{\text{corr}}$ ) were determined by the Tafel line extrapolation. One specimen was used for a measurement, with the potential scan of  $0.5 \text{ mV s}^{-1}$ , from the cathodic to the anodic region. The polarization resistance ( $R_p$ ) values were determined from liner polarization measurements, which were performed between  $\pm 10 \text{ mV}$  around  $E_{\text{corr}}$ , after immersion for 1 h in the base solution, with a scan rate of  $0.1 \text{ mV s}^{-1}$ .

The measurements of electrochemical impedance spectra (EIS) were performed at the open circuit potential with the FRA2 module applying a signal of  $10 \text{ mV}$  amplitude in the frequency range  $20 \text{ kHz}$  to  $0.001 \text{ Hz}$ .

## RESULTS AND DISCUSSION

### Composition and surface morphology

Four phosphating solutions of different composition: PZn, PZnCa, PZnNi and PZnNiMn were applied to grow protective coatings on the carbon steel surface. It was established in our previous work [25] that during phosphate coating formation on steel surface PZnNi produced heavy weight ( $10\text{--}12 \text{ g m}^{-2}$ ), while PZn, PZnCa and PZnNiMn yielded middle-weight ( $1.7\text{--}8 \text{ g m}^{-2}$ ) crystalline coatings. There is a relation between film density and surface weight, of about  $1 \mu\text{m}$  corresponding to  $1.5\text{--}2 \text{ g m}^{-2}$  for most phosphate coatings [22]. The difference in the surface morphology of the phosphate coatings can be observed from SEM images presented in Fig. 1. The monocation PZn coating appeared to be compact, consisting of platelet shaped crystallites of  $5\text{--}10 \mu\text{m}$  in length and  $2\text{--}3 \mu\text{m}$  in width, which uniformly covered the surface of the sample. The presence of Ca, Ni and Mn ions in the phosphating solutions resulted in the modification of the crystallite form. The bication PZnCa coating is smoother than the monocation PZn coating and its structure is characterized by platelets with sizes up to  $30 \mu\text{m}$  in length, while the bication PZnNi coating consists of larger platelets, the dimensions of which varied between  $10$

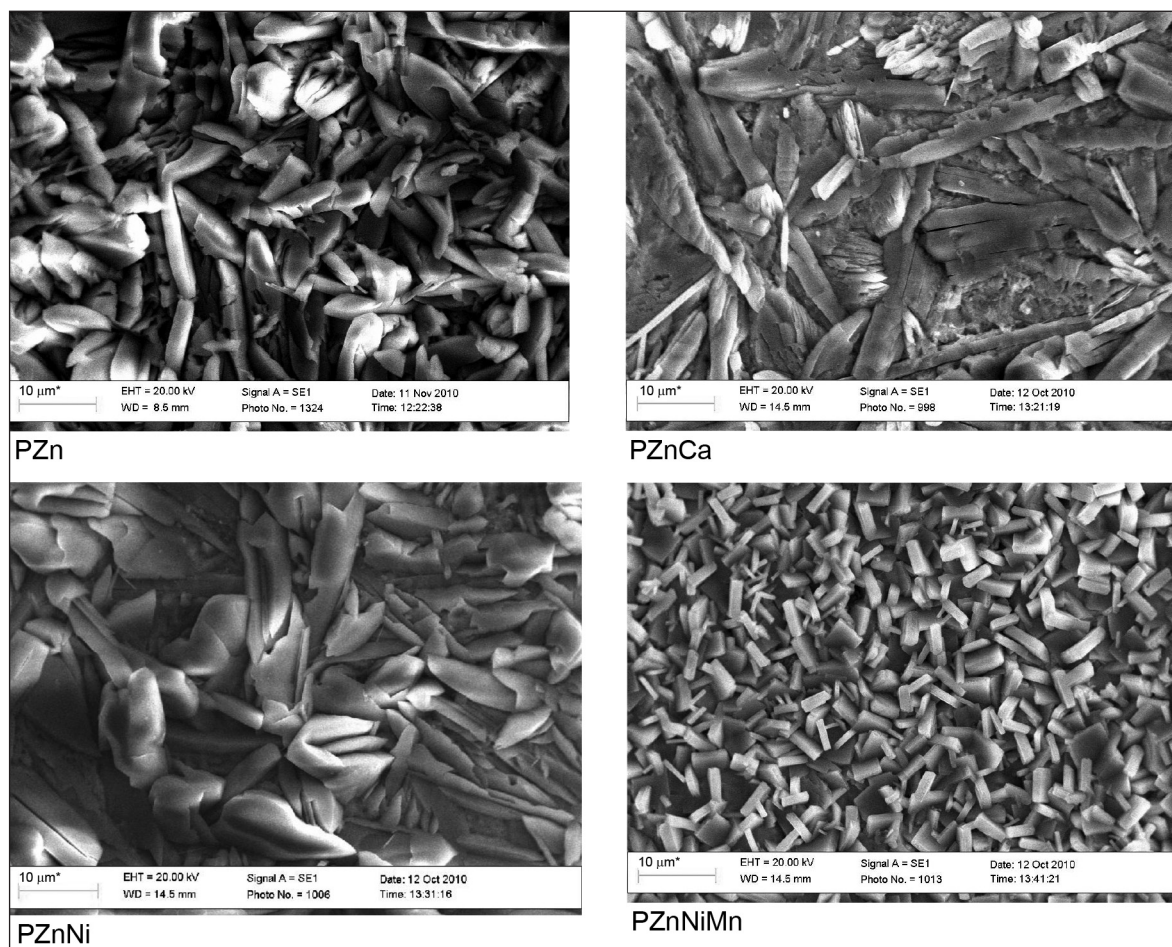


Fig. 1. SEM micrographs of the crystalline phosphate coatings on the carbon steel surface

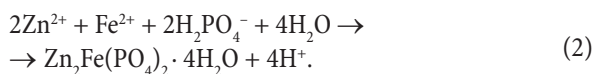
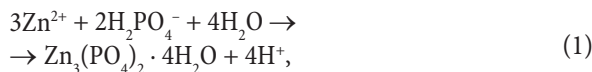
Table 2. Phosphate coating thickness and elemental composition

Phosphate coating	Coating thickness, $\mu\text{m}$ (by XRD)	Elements, at.% (by EDX)						
		Zn	Ca	Ni	Mn	Fe	O	P
PZn	3.7	21.7	–	–	–	3.6	62.4	12.3
PZnCa	1.5–1.8	15.1	0.1	–	–	11.3	61.9	11.6
PZnNi	5.8	19.4	–	0.1	–	3.4	64.0	13.2
PZnNiMn	1.5	9.9	–	0.4	1.1	9.8	67.5	11.3

and 40  $\mu\text{m}$ . The trication PZnNiMn coating is compact, well crystallized and it completely covers the steel surface and its structure is characterized by right-angled crystallites whose width is about 0.1–0.2  $\mu\text{m}$  and length is 2–4  $\mu\text{m}$ .

According to XRD measurements (Fig. 2) all investigated phosphate coatings were mainly composed of the same compounds, as the obtained diffractograms exhibited sharp peaks corresponding to hopeite  $\text{Zn}_3(\text{PO}_4)_2 \cdot 4\text{H}_2\text{O}$ , phosphophyllite  $\text{Zn}_2\text{Fe}(\text{PO}_4)_2 \cdot 4\text{H}_2\text{O}$  and the substrate metal Fe.

The presence of the phosphophyllite phase is related to the carbon steel dissolution in the acid bath (pH = 3.2–3.6) during the phosphate treatment [11]. According to [19], the possible reactions for the hopeite and phosphophyllite formation are as follows:



The intensities of diffraction lines are proportional both to the volume fraction of phosphate phase and the thickness of the phosphate layer [26]. Therefore, the comparison of the intensities of metallic Fe diffraction lines of samples without/with a phosphate layer suggests that the thickness

of the crystalline phosphate coatings formed on the surface of carbon steel increased in the following order: PZnNiMn, PZnCa < PZn < PZnNi (Table 2).

The analysis of elemental composition of the phosphate coatings, which was performed by EDX measurements and the results of which are listed in Table 2, indicated that PZnCa and PZnNi coatings contained only 0.1 at.% of Ca or Ni while PZnNiMn contained 0.4 at.% of Ni and 1.1 at.% of Mn. Besides, the latter phosphate coating contained the lowest amount of Zn (~9.9 at.%), with respect to the other three coatings, which contained from 15.1 to 21.7 at.% of Zn.

#### Polarization measurements

The detrimental effect of chloride ions on the passive layer formed on iron exposed to alkaline environments has been reported extensively in literature [3, 12, 25, 27]. The influence of  $\text{Cl}^-$  ions on the passivity breakdown of carbon steel can be interpreted as a balance between two processes competing on the metal surface: stabilization of the passive film by  $\text{OH}^-$  adsorption and disruption of the film by  $\text{Cl}^-$  ions adsorption. When the activity of chlorides overcomes that of hydroxyls, pitting occurs. Therefore, an aggressive solution, the saturated  $\text{Ca}(\text{OH})_2 + 1 \text{ M NaCl}$  (base), was selected for further studies.

The variation in  $E_{\text{corr}}$  values in the base solution for unphosphated and phosphated carbon steel samples is shown in Fig. 3. According to the electrochemical theory, the free corrosion

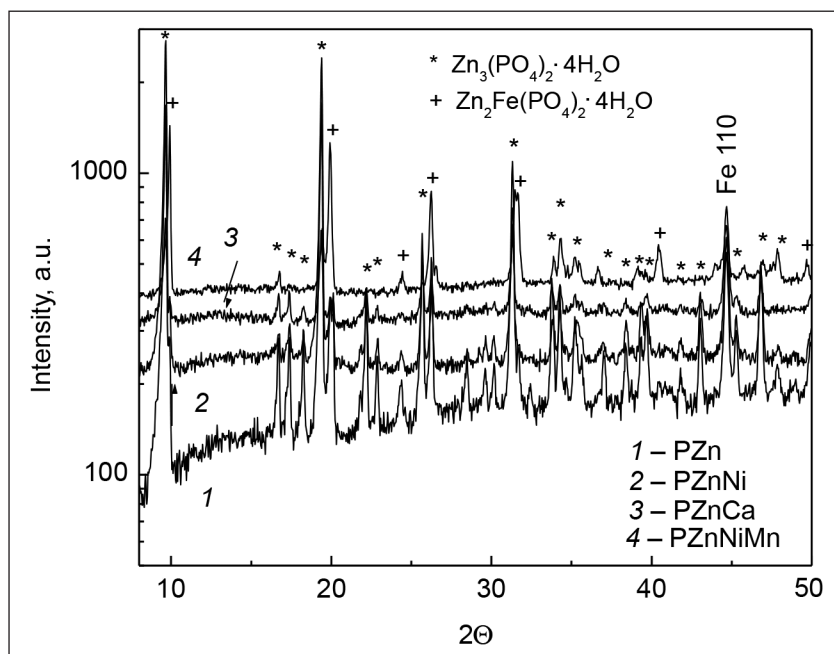


Fig. 2. XRD patterns of the phosphate coatings on carbon steel

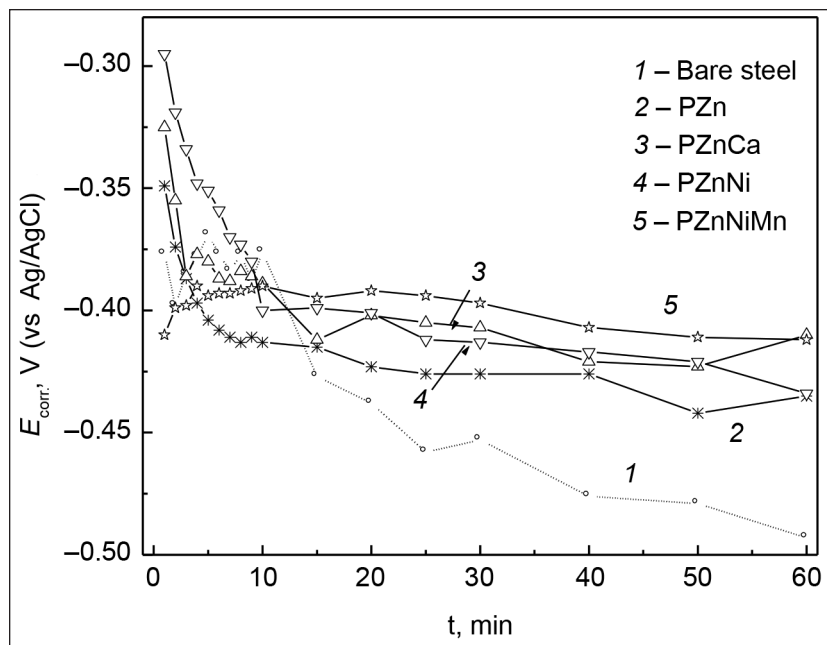


Fig. 3. Dependence of the corrosion potential ( $E_{\text{corr}}$ ) of the carbon steel electrode without/with phosphate coatings in a sat.  $\text{Ca}(\text{OH})_2 + 1 \text{ M NaCl}$  solution on the time of exposure at  $25^\circ\text{C}$

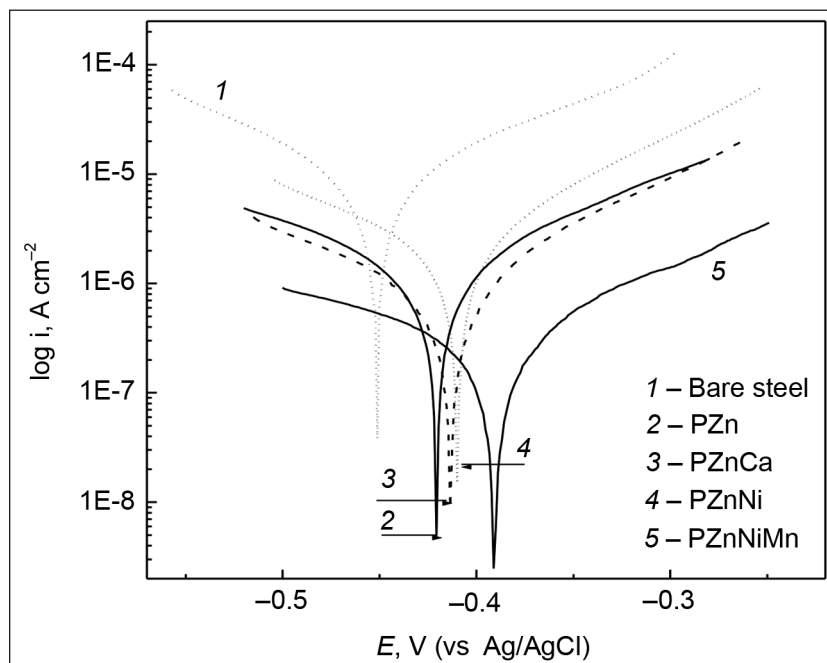


Fig. 4. Potentiodynamic polarization curves of the carbon steel electrodes without/with the phosphate coatings measured after immersion in a sat.  $\text{Ca}(\text{OH})_2 + 1 \text{ M NaCl}$  solution for 1 h at  $25^\circ\text{C}$ ;  $0.5 \text{ mV s}^{-1}$

potential is the mixed potential between local anodic and cathodic reaction during an electrochemical corrosion process. The most rapid evolution of  $E_{\text{corr}}$  occurred within  $\sim 20$  min of the sample immersion, while further potential evolution was slower and did not change significantly. Therefore,  $E_{\text{corr}}$  values were monitored during one-hour period. The data obtained have shown that  $E_{\text{corr}}$  values of all samples with the crystalline phosphate coatings exhibited more positive potentials as compared to those of unphosphated substrates (Table 3).

The polarization curves of the carbon steel electrode without/with phosphate coatings are shown in Fig. 4. During the polarization process the properties of the substrate material do not change so the anodic process of the coated sample is the same as that of the non-coated one. However, due to the barrier effect of the phosphate coating, the average polarization current declines considerably as compared to the bare steel characteristics. The values of  $i_{\text{corr}}$  and  $R_p$  were determined from polarization measurements and the results obtained are listed in Table 3. As seen from the data presented in Table 3, among all the investigated coatings the PZnNiMn samples exhibited the lowest values of  $i_{\text{corr}} = 1.5 \cdot 10^{-7} \text{ A cm}^{-2}$  and the highest values of  $R_p = 59 \text{ k}\Omega \text{ cm}^2$ , while PZnNi samples possessed the highest  $i_{\text{corr}} = 7.2 \cdot 10^{-7} \text{ A cm}^{-2}$  and the smallest  $R_p = 16.5 \text{ k}\Omega \text{ cm}^2$ . For the samples with PZnNiMn coating the values of  $i_{\text{corr}}$  were found to be twenty-fold lower and values of  $R_p$  were seventeen-fold higher with respect to those of bare steel.

The protection efficiency  $P\%$  (Table 4) of phosphate coatings was calculated using the following equation [22]:

Table 3. The electrochemical parameters of carbon steel with / without the phosphate coatings after 1 h immersion in a sat.  $\text{Ca}(\text{OH})_2 + 1 \text{ M NaCl}$  solution

Sample	Electrochemical parameters (Linear polarization technique)			
	$E_{\text{corr}}$ V (vs Ag/AgCl)	$\Delta E_{\text{corr}}$ V	$i_{\text{corr}}$ A $\text{cm}^{-2}$	$R_p$ $\text{k}\Omega \text{ cm}^2$
Bare steel	-0.452	-	$3.2 \cdot 10^{-6}$	3.5
PZn	-0.420	0.032	$3.6 \cdot 10^{-7}$	52.7
PZnCa	-0.414	0.038	$3.1 \cdot 10^{-7}$	54.5
PZnNi	-0.412	0.040	$7.2 \cdot 10^{-7}$	16.5
PZnNiMn	-0.391	0.061	$1.5 \cdot 10^{-7}$	59

Table 4. Porosity ( $F$ ), protection efficiency ( $P\%$ ) and ratios of polarization resistances  $R_{\text{unph}}/R_{\text{ph}}$ , where  $R_{\text{unph}}$  and  $R_{\text{ph}}$  denote the polarization resistance of unphosphated and phosphated carbon steel, respectively

Phosphate coating	Linear polarization technique			Electrochemical impedance technique		
	$F, \%$	$P\%$	$R_{\text{unph}}/R_{\text{ph}}$	$F, \%$	$P\%$	$R_{\text{unph}}/R_{\text{ph}}$
PZn	2.6	93.4	0.066	2.8	94.3	0.072
PZnCa	2.1	93.6	0.064	2.3	92.8	0.072
PZnNi	6.5	78.8	0.21	7.2	76.5	0.23
PZnNiMn	1.0	94	0.059	0.9	94	0.06

$$P\% = (R_p - R_{p,m}) / R_p, \quad (3)$$

where  $R_{p,m}$  is the polarization resistance of bare steel;  $R_p$  is the polarization resistance of phosphated steel.

The major problem in using protective coatings in aggressive environments is the possible presence of open porosity and pinholes in the coatings [10]. These local defects form direct paths between the corrosive environment and substrate. As the corrosion reactions are initiated at the coating-substrate interface, determination of the porosity is essential in order to estimate the overall corrosion resistance of the coated sample. On the assumption that the phosphate coating is electrochemically inert at low anodic overpotentials, the total porosity ( $F$ ) of the coating was calculated using the following equation [19–21]:

$$F = (R_{p,m}/R_p) \times 10^{-\Delta E_{\text{corr}}/b_a}, \quad (4)$$

where  $R_{p,m}$  is the polarization resistance of bare steel;  $R_p$  is the polarization resistance of phosphated steel;  $\Delta E_{\text{corr}}$  is the difference of  $E_{\text{corr}}$  between steel electrodes with and without phosphate coatings;  $b_a$  is the anodic Tafel slope for bare steel. The carbon steel electrode possessed the following characteristics:  $b_a = 78$  mV and  $R_{p,m} = 3.5$  k $\Omega$  cm<sup>2</sup>.

The porosity was evaluated in terms of surface ratio between the substrate surface in contact with the solution through the open porosity and the coating surface. It has been established that  $F$  of the ZnNiMn sample was of the order of 1% while that of PZnNi was ca. sevenfold higher (6.5%). The obtained values of porosity are in good agreement with the results of corrosion behaviour ( $i_{\text{corr}}$  and  $R_p$  values) of phosphated carbon steel samples in the investigated solution (Tables 3 and 4). Carbon steel samples coated with ZnNiMn exhibited the lowest values of  $i_{\text{corr}}$ , the highest  $R_p$  and the lowest  $F$ . The results obtained imply that the thickness of the phosphate coating (Table 2) does not have crucial influence on the corrosion parameters  $i_{\text{corr}}$  and  $R_p$  (Table 3). X-ray diffraction measurements indicated that although the thickness of the PZnNiMn coating was the smallest one ( $\leq 2$   $\mu$ m), it exhibited the lowest  $i_{\text{corr}}$  and the highest  $R_p$  values. The data obtained indicate that the protective abilities of the phosphate coatings depend mainly on the coating porosity.

According to Weng et al. [22], the porosity is directly responsible for the exposed area of substrate at the pores within the coating. The calculated average porosity of PZnNiMn was approximately 1% (Table 3), whereas the  $i_{\text{corr}}$

values of phosphated samples decreased only about twenty-fold as compared to those of bare steel. It means that the steel surface at the bottom of the phosphate coating pores is more active than the surface of bare steel.

### Electrochemical impedance spectroscopy analysis

EIS measurements were carried out with the aim to determine  $R_p$ , which is in the inverse proportion to  $i_{\text{corr}}$ , and to estimate  $F$  of phosphate coatings. EIS diagrams for carbon steel samples without / with phosphate coatings exposed for 1 h to the base solution are given in Fig. 5. The data obtained were fitted and

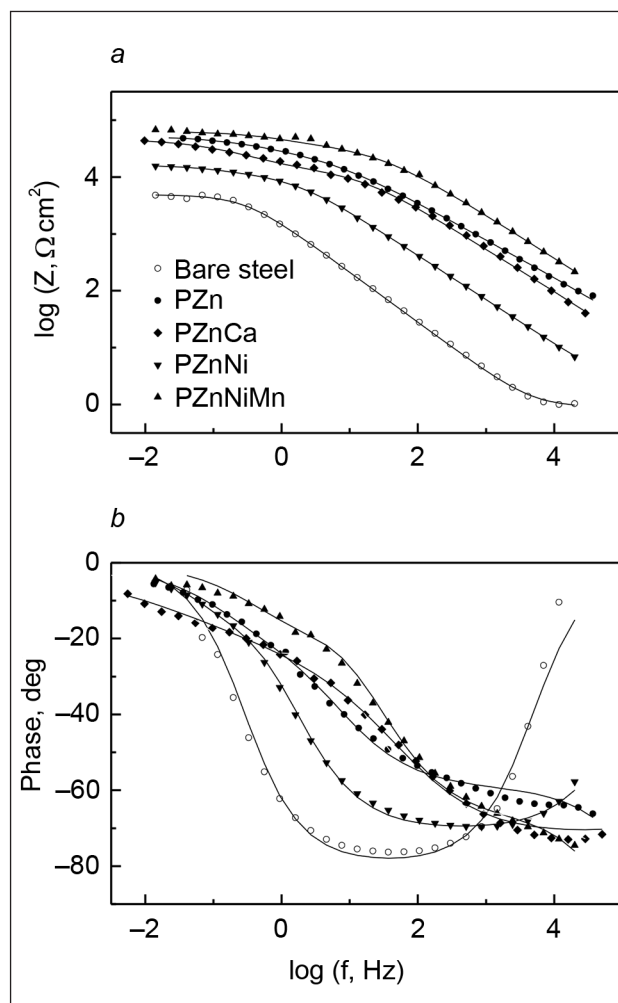


Fig. 5. Bode plots of the impedance spectra after immersion of carbon steel without / with the phosphate coatings in a sat.  $\text{Ca}(\text{OH})_2 + 1$  M NaCl solution for 1 h at 25 °C

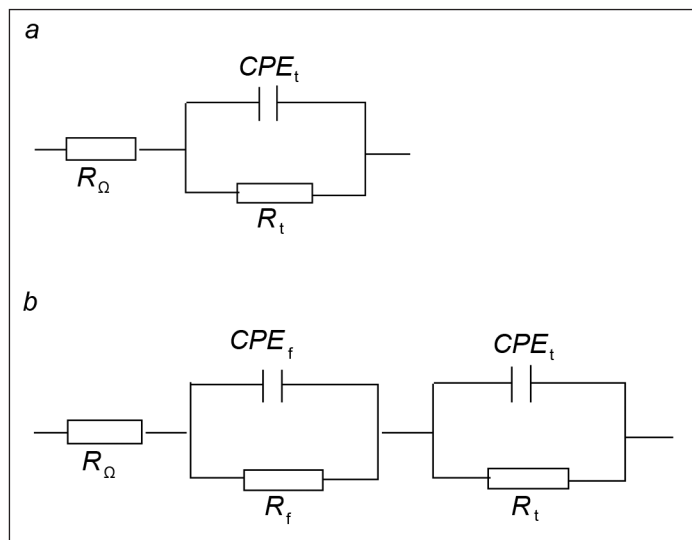


Fig. 6. Equivalent circuits (a) and (b) used for simulation of experimental data.  $R_\Omega$  – the resistance of the solution;  $R_t$ ,  $CPE_t$  – the charge transfer resistance and the constant phase element;  $R_f$ ,  $CPE_f$  – the electrical resistance of ion transfer through open phosphate coating pores and the constant phase element

analysed using the EQUIVCRT program of Boukamp [28]. To interpret the EIS data, two equivalent circuit models that are generally used to describe corrosion processes (Fig. 6) [29, 30] were applied. The calculated parameters of equivalent circuit were used for simulation of impedance diagrams.

The electrical parameters obtained for non-phosphated carbon steel through fitting EIS data using an electrical equivalent circuit ( $R_\Omega(Q_tR_t)$ ) are listed in Table 5. The proposed electric equivalent circuit is given in Fig. 6a, where  $R_\Omega = 1\text{--}2 \Omega \text{ cm}^2$  corresponds to the electrolyte resistance between the working and reference electrodes,  $R_t$  represents the charge transfer resistance of the steel/solution interface,  $Q$  is the constant phase element (CPE). CPE was used instead of a simple capacitor (C) and it is defined by the admittance  $Y$  and the power index number  $n$ :

$$Y = Y_0(j\omega)^n, \quad (5)$$

where  $j$  is the imaginary unit,  $\omega$  is the angular frequency. The term  $n$  shows how far the interface is from the ideal capacitor (C). When the value of  $n$  is equal to 1, the distributed element is a pure capacitor, if  $n$  is close to 0.5, the distributed element is pure Warburg impedance, if  $n$  is zero, the distributed

element is a pure resistance. In the present measurements,  $n$  was in most cases from 0.88 down to 0.64. This indicates that the system behaves like a leaky capacitor; values of about 0.65 indicate a prevailing contribution of transport control [31].

Impedance spectra recorded for phosphated steel samples show the best fit to the  $R_\Omega(Q_fR_f)(Q_tR_t)$  circuit (Fig. 6b). The first in series  $R_f$ - $CPE_f$  combination should represent the resistance and capacitance of the phosphate coating, where  $R_f$  is the electrical resistance of ion transfer through the open coating pores in parallel with coating capacitance. The second  $R_t$ - $CPE_t$  is related to the electrochemical properties of the corroding steel electrode. The fitting parameters are listed in Table 5. The phosphated samples exhibited lower  $Y_0(Q_t)$  and higher  $R_t$  than those of bare steel. The higher  $R_t$  values correlated with more noble open-circuit potentials for the phosphated samples as compared with those of unphosphated substrate (Tables 3, 5).  $R_t$  increased for the investigated samples in the order: bare steel  $\leq$  PZnNi  $\leq$  PZnCa, PZn  $\leq$  PZnNiMn, showing a relation between corrosion resistance of the samples, in which PZnNiMn is more corrosion resistant than the others.

The carbon steel samples covered with the phosphate coatings possessed from four- to seventeen-fold higher po-

Table 5. Electrochemical impedance spectroscopy parameters obtained by fitting the Bode plots shown in Fig. 5 with equivalent circuits shown in Fig. 6 for carbon steel without / with the phosphate coatings measured after exposure for 1 h to a sat.  $\text{Ca}(\text{OH})_2 + 1 \text{ M NaCl}$  solution;  $R_\Omega = 1\text{--}2 \Omega \text{ cm}^2$

Phosphate coating	$R_p$ , $\text{k}\Omega \text{ cm}^2$	$Y_0(Q_t) \times 10^6$ , $\Omega^{-1} \text{ cm}^{-2} \text{ s}^n$	$n(Q_t)$	$R_p$ , $\text{k}\Omega \text{ cm}^2$	$Y_0(Q_t) \times 10^6$ , $\Omega^{-1} \text{ cm}^{-2} \text{ s}^n$	$n(Q_t)$	$^*R_p$ , $\text{k}\Omega \text{ cm}^2$	$\chi^2$ (error factor)
Bare steel	3.8	121	0.88	–	–	–	3.8	0.0041
PZn	18.9	4.8	0.7	34.1	18.6	0.64	53	0.0038
PZnCa	17.6	2.8	0.8	34.9	33	0.65	52.5	0.0024
PZnNi	5.5	37.8	0.8	10.7	16.1	0.76	16.2	0.0037
PZnNiMn	28.8	2.3	0.8	34.9	9.1	0.66	63.7	0.0051

$$^*R_p = R_t + R_f + R_\Omega.$$

larization resistance ( $R_p = R_f + R_t + R_\Omega$ ) values as compared to those of bare steel samples. Among the samples with the phosphate coatings, the trication PZnNiMn showed the highest value of  $R_p = 63.7 \text{ k}\Omega \text{ cm}^2$ . The PZnNi showed  $R_p$  values close to  $16.2 \text{ k}\Omega \text{ cm}^2$ , which appeared to be the lowest one from the others studied phosphate coatings.

Characterisation of phosphate coatings involves determination of porosity. The values of porosity of the phosphate coatings were calculated on the basis of determined electrochemical parameters using Eq. (4) and the results obtained are listed in Table 4. It has been established that the porosity of the PZnNiMn sample was in the order of 1%, while that of the PZnNi sample was ca. sevenfold higher  $\sim 7.2\%$ . The porosity rate values obtained by EIS were in total agreement with the values evaluated by linear polarization measurements.

Porosity can be defined as a ratio of the surface exposed in the pores to the entire surface, and it can be expressed by the ratio:  $R_{\text{unph}}/R_{\text{ph}}$ , where  $R_{\text{unph}}$  and  $R_{\text{ph}}$  denote polarization resistance of unphosphated and phosphated materials, respectively [31]. The ratios were calculated from the average values of the polarization resistances presented in Tables 3 and 5. The ratios of resistances suggest porosity of 6–7% for PZn, PZnCa, PZnNiMn and about 20% for PZnNi. All the values, particularly the value for PZnNi, appeared to be unrealistically high for a true porosity. It can be supposed that electrochemical reactions occur over an area larger than the surface exposed in pores.

The assumption that the mechanism of electrochemical/chemical reaction in pores of phosphate coating and bare metal is the same is often not verified. The free surface at the bottom of the pores was found to be modified in pre-treatment and post-treatment operations and in some cases was found to be more active than the clean bare metal surface [29]. Furthermore, in the pores of coating the anodic reaction is the dissolution of iron, and the cathodic reaction is the depolarization of dissolved oxygen. With the hydrolysis of ferrous ions, the electrolyte in the occluded zone is locally acidified. The damage to the coating also begins close to the metal surface. This leads to the penetration of aggressive medium underneath the coating, causing the corrosion of the substrate spreading along the surface. This is called under-film corrosion of phosphated steel in an aqueous solution [22].

The data obtained indicate that among all investigated samples the least porous ( $F \leq 1\%$ ) PZnNiMn coating exhibited the best protective abilities in a chloride-contaminated alkaline solution.

## CONCLUSIONS

According to XRD analysis data, all investigated phosphate coatings were composed mainly of three phases: hopeite  $\text{Zn}_3(\text{PO}_4)_2 \cdot 4\text{H}_2\text{O}$ , phosphophyllite  $\text{Zn}_2\text{Fe}(\text{PO}_4)_2 \cdot 4\text{H}_2\text{O}$  and the substrate metal Fe. The investigated coatings differed mainly in their elemental composition and surface morphology.

The results of electrochemical measurements revealed that after immersion into a saturated  $\text{Ca}(\text{OH})_2 + 1 \text{ M NaCl}$  solution for 1 h the carbon steel samples covered with the phosphate coatings possessed from four- to seventeen-fold higher  $R_p$  values in comparison to those of bare steel samples.

The porosity rate values obtained by electrochemical impedance spectroscopy (EIS) were in total agreement with the values evaluated by linear polarization measurements.

The electrochemical behaviour of the phosphated carbon steel samples depended mainly on the presence of local defects (porosity) in the coating.

The ratios  $R_{\text{unph}}/R_{\text{ph}}$ , where  $R_{\text{unph}}$  and  $R_{\text{ph}}$  denote polarization resistance of unphosphated and phosphated materials, respectively, are too high to be assigned exclusively to porosity. Evidently, they include processes occurring over an area larger than that of the pores.

To summarize the results of electrochemical and SEM measurements, the low porosity medium weight crystalline PZnNiMn phosphate coating on carbon steel demonstrated effective protective properties in a chloride-contaminated alkaline solution.

## ACKNOWLEDGEMENTS

This research was supported by the Research Council of Lithuania under Grant No. MIP-77/2010. The authors thank dr. A. Selskis (Institute of Chemistry, Centre for Physical Sciences and Technology) for his assistance performing SEM measurements and dr. R. Juškėnas (Institute of Chemistry, Centre for Physical Sciences and Technology) for his assistance performing XRD measurements.

Received 31 July 2013

Accepted 5 September 2013

## References

1. H. Oranowska, Z. Szklarska-Smialowska, *Corr. Sci.*, **21**, 735 (1981).
2. J. T. Hinatsu, W. F. Graydon, F. R. Foulkes, *J. Appl. Electrochem.*, **20**, 841 (1990).
3. L. Li, A. A. Saqués, *Corrosion*, **57**, 19 (2001).
4. U. Angst, B. Elsener, C. K. Larsen, Ø. Vennesland, *Cem. Concr. Res.*, **39**, 1122 (2009).
5. F. Simescu, H. Idrissi, *Corr. Sci.*, **51**, 833 (2009).
6. M. Manna, *Corr. Sci.*, **51**, 451 (2009).
7. O. Girčienė, M. Samulevičienė, V. Burokas, R. Ramanauskas, *Chemija*, **19/1**, 14 (2008).
8. W. Machu, *Die Phosphatierung*, Verlag Chemie (1950).
9. G. Lorin, *Phosphating of Metals*, Finishing Publications Ltd. (1974).
10. A. Neuhaus, M. Gebhardt, *Werkst. Korros.*, **17**, 493 (1966).
11. D. B. Freeman, *Phosphating and Metal Pre-Treatment*, Woodhead-Faulkner Ltd., Cambridge, England (1986).
12. V. F. C. Lins, G. F. A. Reis, C. R. Araujo, T. Matencio, *Appl. Surf. Sci.*, **253**, 2875 (2006).

13. K. Ogle, A. Tomandl, N. Meddahi, M. Wolpers, *Corr. Sci.*, **46**, 979 (2004).
14. A. Tomandl, M. Wolpers, K. Ogle, *Corr. Sci.*, **46**, 997 (2004).
15. H. Gehmecker, *Metalloberfläche*, **44**, 485 (1990).
16. M. M. Jalili, S. Moradian, D. Hosseinpour, *Constr. Build. Mater.*, **23**, 233 (2009).
17. W. Paatsch, W. Kautek, M. Sahre, *Trans. Inst. Met. Finish.*, **75(6)**, 216 (1997).
18. D. Zimmermann, A. G. Munoz, J. W. Schultze, *Electrochim. Acta*, **48**, 3267 (2003).
19. J. Donofrio, *Met. Finish.*, **98**, 57 (2000).
20. M. F. Morks, *Mater. Lett.*, **58**, 3316 (2004).
21. W. A. Roland, K. H. Gottwald, *Metalloberfläche*, **42**, 301 (1988).
22. D. Weng, P. Jokiel, A. Uebleis, H. Boehni, *Surf. Coat. Technol.*, **88**, 147 (1996).
23. J. Creus, H. Mazille, H. Idrissi, *Surf. Coat. Technol.*, **130**, 224 (2000).
24. C. Liu, Q. Bi, A. Leyland, A. Matthews, *Corr. Sci.*, **45**, 1257 (2003).
25. K. Y. Ann, H.-WW. Song, *Corr. Sci.*, **49**, 4113 (2007).
26. B. D. Cullity, *Elements of X-Ray Diffraction*, 2nd edn., P. 285, Addison-Wesley Publishing Company (1978).
27. O. Girčienė, R. Ramanauskas, L. Gudavičiūtė, A. Martušienė, *Corrosion*, **67**, 125001-1 (2011).
28. B. A. Boukamp, *J. Electrochem. Soc.*, **142**, 1885 (1995).
29. L. Freire, X. R. Nóvoa, M. F. Montemor, M. J. Carmezim, *Mater. Chem. Phys.*, **114**, 962 (2009).
30. El-Sayed M. Sherif, R. M. Erasmus, J. D. Comins, *Electrochim. Acta*, **55**, 3657 (2010).
31. J. Flis, Y. Tobiya, K. Mochizuki, C. Shiga, *Corros. Sci.*, **39**, 1757 (1997).

Olga Girčienė, Rimantas Ramanauskas, Laima Gudavičiūtė,  
Aldona Martušienė

#### FOSFATINIŲ DANGŲ SUDĖTIES ĮTAKA ANGLINIO PLIENO APSAUGAI NUO KOROZIJOS CHLORIDAIS UŽTERŠTAME ŠARMINIAME TIRPALE

##### S a n t r a u k a

Ištirta anglinio plieno, padengto įvairios sudėties kristalinėmis fosfatinėmis dangomis Zn (PZn), Zn-Ca (PZnCa), Zn-Ni (PZnNi) ir Zn-Ni-Mn (PZnNiMn), korozinė elgsena chloridais užterštame šarminiame tirpale. Fosfatinių dangų cheminė sudėtis ir morfologija buvo tirtos naudojant rentgeno spindulių difrakcinės (XRD) analizės ir skenuojančios elektronų mikroskopijos (SEM) metodus, o korozijos ir poringumo parametrai buvo įvertinti atlikus elektrocheminius matavimus. Nustatyta, kad visos tirtos konversinės dangos sudarytos iš trijų fazių: hopeito  $Zn_3(PO_4)_2 \cdot 4H_2O$ , fosfofilito  $Zn_2Fe(PO_4)_2 \cdot 4H_2O$  ir substrato metalo Fe. Atlikti elektrocheminiai matavimai parodė, kad 1 val. laikytų sočiame  $Ca(OH)_2 + 1 M NaCl$  tirpale elektrodų, padengtų fosfatinėmis dangomis, poliarizacinių varžų ( $R_p$ ) vertės yra nuo keturių iki septyniolikos kartų didesnės nei plieninių bandinių. Poringumų vertės, nustatytos elektrocheminio impedanso spektroskopijos metodu (EIS), yra labai artimos vertėms, apskaičiuotoms pagal poliarizacinių matavimų duomenis. Nustatyta, kad mažo poringumo PZnNiMn fosfatinė danga, nusodinta ant anglinio plieno, pasižymi geriausiomis apsauginėmis savybėmis šarminiame chloridais užterštame tirpale.